

## THERMAL DECOMPOSITION OF DYSPROSIUM IRON CITRATE

V.K. SANKARANARAYANAN and N.S. GAJBHIYE

*Department of Chemistry, Indian Institute of Technology, Kanpur 208 016 (India)*

(Received 16 March 1989)

### ABSTRACT

The citrate gel process was used to synthesize ultrafine-grained, amorphous and crystalline  $\text{Dy}_3\text{Fe}_5\text{O}_{12}$  (dysprosium iron garnet, DyIG). The citrate precursor is obtained on drying the citrate gel at  $110^\circ\text{C}$  and has the chemical composition  $\text{Dy}_3\text{Fe}_5(\text{Cit})_{25} \cdot 36\text{H}_2\text{O}$ . The thermal decomposition of the hydrated citrate precursor was investigated by DTA, TG and DSC techniques, and gas and chemical analyses. An air atmosphere is found to be most suitable for the decomposition yielding stoichiometric DyIG. The decomposition consists of six steps. The dehydration step of the citrate precursor is followed by a low temperature decomposition of the citrate groups. The formation of a transient intermediate containing both citrate and carbonate groups is associated with evolution of  $\text{CO}$ ,  $\text{CO}_2$ , water vapour and the burning-off of methylene groups in the temperature range  $160\text{--}280^\circ\text{C}$ . The citrate groups are completely destroyed in the temperature range  $280\text{--}330^\circ\text{C}$  resulting in the formation of a carbonate which retains free  $\text{CO}_2$  gas in the matrix. The final decomposition of the carbonate takes place between  $330$  and  $450^\circ\text{C}$  and yields ultrafine-grained amorphous DyIG, releases the trapped  $\text{CO}_2$  above  $450^\circ\text{C}$  and crystallizes at  $590^\circ\text{C}$ . The citrate precursor and decomposed products were characterized by IR and NMR spectra, X-ray diffraction data and surface area measurements.

### INTRODUCTION

Technologically, rare earth–iron garnet materials are of vital interest due to their applications in bubble domain and microwave devices. This has prompted the development of various chemical methods, which include coprecipitation, freeze drying, spray drying and sol-gel, in the preparation of stoichiometric and chemically pure rare earth–iron garnet materials [1–3]. In particular, the citrate gel process has been shown to have great potential in the preparation of rare earth iron garnets. In the citrate-gel method, hydrated dysprosium iron citrate precursor is prepared by adding a polyfunctional hydroxy acid such as citric acid to a solution containing metal salts of dysprosium and iron. Dysprosium iron garnet (DyIG) is obtained by the thermal decomposition of hydrated dysprosium iron citrate (citrate precursor). The reactivity of the end product and its particle size are signifi-

cantly influenced by the calcination temperature. Consequently, the thermal decomposition of the citrate precursor has special significance.

A literature survey showed that no systematic efforts have been made to investigate the thermal decomposition of rare earth-iron citrate materials, and studies do not report the decomposition of the dysprosium iron citrate precursor. Thermal decomposition studies of ferrites including  $Y_3Fe_5O_{12}$  and  $Y_3Al_5O_{12}$  garnets prepared by the citrate method are not comprehensive and remain inconclusive [4,5]. Thus the nature of the final product may be altered. The present investigation was undertaken to study the mode of thermal decomposition of the hydrated dysprosium iron citrate precursor. These studies enable us to explain all the observed facts regarding the thermal decomposition of hydrated citrate precursor and to propose a logical scheme for this multi-stage decomposition.

## EXPERIMENTAL

### *Preparation of the dysprosium iron citrate precursor*

Dysprosium oxide (11.5650 g),  $Dy_2O_3$  (Metals Research Ltd., 99.999% pure), was accurately weighed out and dissolved in 50 ml of AnalaR 6N nitric acid (IDPL). After a clear solution of dysprosium nitrate was formed, the solution was evaporated to dryness and dissolved in 50 ml of distilled water. This solution was repeatedly evaporated to dryness to make sure that excess nitric acid was removed. Ferric citrate (32.4210 g; Aldrich and Thomas) was dissolved in a minimum amount of warm distilled water with constant stirring and added to the dysprosium nitrate solution. Citric acid (104 g; S.D. AnalaR) was dissolved in 100 ml of water in a separate beaker and added to the above solution. The solution, containing dysprosium nitrate, ferric citrate and citric acid, was transferred into a 500 ml round-bottomed flask. The resultant homogeneous solution was refluxed for 12 h at  $100^\circ C$ . Finally, the refluxed solution was slowly evaporated to concentrate it and then transferred to a Petri dish to form a gel. The gel was dehydrated in an oven at  $110^\circ C$  to obtain the dysprosium iron citrate and to ensure the complete removal of excess water and nitric acid. During this process, the gel swells into a fluffy chocolate-coloured mass, which eventually breaks down to brittle flakes. The precursor contains more water molecules than the hydrated citrate precursor. Wet chemical analysis of this citrate precursor established the stoichiometric formula  $Dy_3Fe_5(Cit)_{25} \cdot 36H_2O$ . Chemical analysis gave: Dy, 7.9; Fe, 4.52; citrate, 76.9 and  $H_2O$ , 10.5%. The calculated values for  $D_3Fe_5(Cit)_{25} \cdot 36H_2O$  are: Dy, 7.94; Fe, 4.55; citrate, 76.96 and  $H_2O$ , 10.55%. This precursor is hygroscopic in nature and absorbs water molecules on standing open in an air atmosphere.

## *Thermal analysis*

Thermal analyses of the citrate precursor were carried out up to 1000 °C with a Linseis Model L81/042 derivatograph, which records DTA and TG simultaneously. Samples of 100 mg were placed in platinum crucibles; ignited alumina was used as the reference material with a heating rate of 5 ° min<sup>-1</sup>. Thermal analyses were carried out in an air atmosphere. DSC and derivative DSC were recorded on a Du Pont 910 differential scanning calorimeter up to 600 °C.

A Perkin–Elmer 240C elemental analyser was used to analyse the evolved gases.

The IR spectra were recorded with a Perkin–Elmer model 377 IR spectrophotometer in the range 4000–400 cm<sup>-1</sup> using samples in the form of KBr pellets.

Proton NMR spectra were recorded using a Bruker model WP80 NMR spectrometer using deuterated DMSO as the solvent.

X-ray diffractograms were recorded using a Rich Seifert Isodebyflex X-ray unit model 2002 with Cu *K*α radiation and a nickel filter.

Surface area measurements of residues were measured by the single point BET method with a Quantachrome Quantasorb Sorption System model QS-7 using nitrogen gas as the adsorber.

## RESULTS

### *Effect of atmosphere on thermal decomposition*

To optimize the effect of the atmosphere, the decomposition of the citrate precursor was carried out in different atmospheres. The compositions of nitrogen and oxygen in the atmospheres were in the ratio: (a) 00 : 100 (dry oxygen), (b) 50 : 50, (c) 80 : 20 (air) and (d) 100 : 00 (dry nitrogen). The citrate precursor was initially decomposed at 450 °C for 24 h in these four different atmospheres. The final heat treatment to these samples was in air for 4 h. Heat treatment above 600 °C leads to crystallization of the DyIG phase. All the resultant samples were found to be X-ray amorphous when heat treated below 600 °C irrespective of the atmosphere employed for decomposition. The lattice parameters calculated for these samples when heat treated in air at 700 °C after decomposing in atmospheres (a)–(d), were 12.3781, 12.3950, 12.4090 and 12.400 Å, respectively. Pure air and pure nitrogen atmosphere heat-treated samples show lattice parameters that are very close to the value of 12.4050 Å for DyIG. Figure 1 shows the IR spectra of these heat-treated samples at 700 °C. The presence of better defined DyIG absorptions are observed for the samples decomposed in air and nitrogen atmosphere. It is important to note that the sample decomposed in

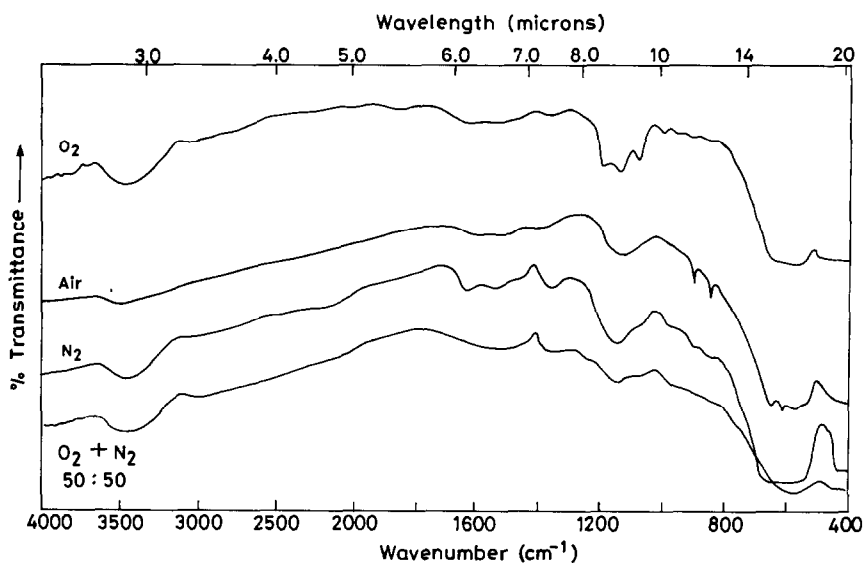


Fig. 1. IR spectra of decomposed dysprosium iron citrate precursor in various atmospheres.

air atmosphere has well-defined DyIG peaks compared with the sample decomposed in nitrogen atmosphere. The above observations lead us to conclude that the initial decomposition carried out in an air atmosphere gives the best results for the crystallization of pure DyIG phase. As a result, the thermal decomposition studies were carried out in air atmosphere. However, it is evident from the studies that a larger percentage of oxygen in the surrounding atmosphere during thermal decomposition leads to vigorous inhomogeneous oxidation reactions resulting in the formation of orthoferrite and  $\text{Fe}_2\text{O}_3$  as extra phases and abnormalities in the DyIG lattice.

#### *Thermal decomposition of the citrate precursor*

TG and DTA curves are shown in Fig. 2 and DSC and derivative DSC curves are shown in Fig. 3, which were recorded in air atmosphere. It can be seen that a one-to-one correlation exists between the DSC and TG curves indicating that the thermal effects are accompanied by weight losses. There are three major steps in the decomposition, the probable reactions being: (i) dehydration, (ii) decomposition of citrate to complex carbonates and (iii) decomposition of carbonates to dysprosium iron garnet. There are two endothermic peaks corresponding to dehydration of the citrate precursor. After dehydration there are three endothermic peaks corresponding to citrate decomposition followed by an endothermic peak corresponding to DyIG formation. The complete data for the observed weight losses and the corresponding temperature ranges are given in Table 1.

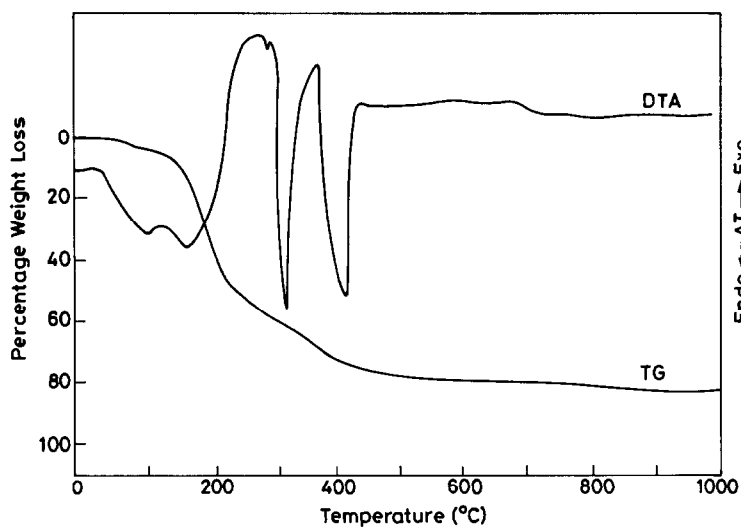


Fig. 2. TG and DTA of dysprosium iron citrate precursor.

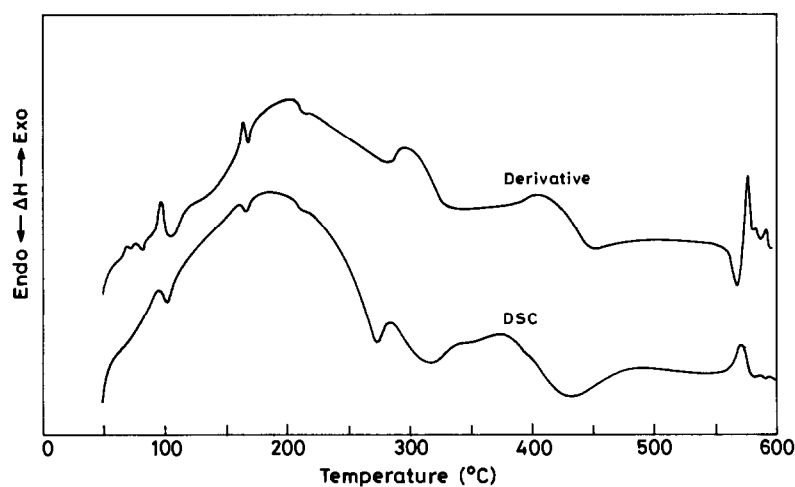


Fig. 3. DSC and derivative-DSC of dysprosium iron citrate precursor.

TABLE 1  
Weight losses in decomposition steps of  $\text{Dy}_3\text{Fe}_5(\text{Cit})_{25} \cdot (36 + n)\text{H}_2\text{O}$

Decomposition step	Temp. range (°C)	Observed wt. loss (%)	Calculated wt. loss (%)
1	25–110	5–15	–
2	110–170	10.2	10.6
3	170–280	61.3	61.5
4	280–330	5.8	5.5
5	330–450	4.0	3.7
6	> 450	2.5	2.8

### *Dehydration of the citrate precursor*

As mentioned earlier, the amount of excess water in the citrate precursor varies depending on the atmospheric humidity. Apart from the 36 coordinated water molecules, the excess water varies from 5 to 15%. The extra water can be removed by heating the citrate precursor at 100 °C, which is shown by the endotherm between 95 and 100 °C (Fig. 2). Dehydration of the citrate precursor takes place between 120 and 170 °C with a maximum around 165 °C, as shown by the second endotherm in Fig. 2. The thermograms show a range of 10–15% weight loss. The actual weight loss due to dehydration alone cannot be independently determined in this range because the decomposition of dysprosium iron citrate precursor sets in around this temperature as shown in Figs. 2 and 3. The coordinated water molecules should be: 15 H<sub>2</sub>O from 5 trihydrated ferric citrate molecules and 21 H<sub>2</sub>O from 21 monohydrated citric acid molecules, giving a total of 36 H<sub>2</sub>O molecules, which amounts to approximately 10% weight loss. While the number of coordinated water molecules in the citrate precursor need not be related to this amount, the weight loss due to dehydration is found to be in the range 10–11%. The temperature range mentioned above is valid only when the pressure is 1 atm.

### *Decomposition of the citrate precursor*

The thermal decomposition of dysprosium iron citrate precursor is a multi-step process. In the temperature range 170–280 °C, the major citrate decomposition occurs with a weight loss of 61% as shown by the thermoanalytical experiments (Table 1). There is evolution of large amounts of carbon monoxide gas, which makes the process exothermic. However, it appears as a shoulder-like endotherm at 220 °C in Fig. 3. The comparatively low temperature required for the side reaction of carbon monoxide formation and the relatively high water vapour pressure during this decomposition are the likely reasons for this step remaining endothermic in air, as reported in the literature [6]. This stage appears as a broad endothermic peak in Figs. 2 and 3. At this stage, citrate precursor decomposition is a complex set of reactions which involves dissociation of the citrate including decarboxylation with evolution of carbon monoxide gas and the oxidation of carbon in air produced during the disproportionation of carbon monoxide. The burning of methylene hydrogens cause the evolution of water vapour. The residue at this stage has a complex structure with citrates partially decomposed to an intermediate structure that retains some of the carboxylate groups. An endotherm appears at 275 °C in the DSC studies (Fig. 3), which indicates the formation of complex carbonates. When the residue obtained is dissolved in conc. HCl, black particles of carbon remain undissolved and this confirms the presence of carbon in samples heated to higher temperatures. The residue at this stage has the apparent composition Dy<sub>3</sub>Fe<sub>5</sub>(COO)<sub>16</sub> ·

$(\text{CO}_3)_2(\text{CO}_2)_2$ , still retaining some of the carboxylate groups with carbonates and traces of carbon dioxide trapped in the lattice.

There are two endothermic peaks noted at 330 and 440 °C. At 330 °C, the structure consists of complex carbonates and trapped  $\text{CO}_2$  gas only, with an apparent composition  $\text{Dy}_3\text{Fe}_5\text{O}_6(\text{CO}_3)_6 \cdot (\text{CO}_2)_3$ . The intermediate complex carbonates decompose between 330 and 440 °C with release of carbon dioxide gas. This thermal decomposition is indicated by an asymmetric peak accompanied by a weight loss of ~ 4%. The composition of this residue after 440 °C is  $\text{Dy}_3\text{Fe}_5\text{O}_{12}(\text{CO}_2)_4$ . Isothermal heating of the citrate precursor at 330 and 440 °C over 2 days yields a residue of the above constant composition with a total weight loss of 81% compared with the 81.5% calculated for the above composition. This residue is DyIG, in an amorphous form with some trapped carbon dioxides and small amounts of residual carbon. Between 450 and 600 °C, negligible weight loss occurs. An overall weight loss of 2–2.5% is observed beyond 450 °C, which corresponds to the release of trapped carbon dioxide and burning of residual carbon.

### *IR spectral studies of citrate precursor decomposition*

The assignment of IR bands is shown in Tables 2 and 3. It appears that the citrate precursor has all the common bands of citric acid and ferric citrate which are listed in Table 2. There are some bands that differ in intensity and are broader in nature indicating the formation of hydrated citrate precursor. The band in the region 3600–3000  $\text{cm}^{-1}$  could be due to the presence of water because the intensity of this absorption decreases and disappears as the heat treatment temperature increases. Similarly the bend-

TABLE 2  
IR spectral frequency assignments of various compounds

Citric acid	Ferric citrate	Precursor $\text{Dy}_3\text{Fe}_5(\text{Cit})_{25} \cdot (36 + n)\text{H}_2\text{O}$	Assignments
3450sh	–	–	$\nu(\text{OH})$ hydroxyl
3300s	3300s	3700–3000vs	$\nu(\text{OH})$ water
2900–2800s	2900–2800s	2900s	$\nu(\text{C}-\text{H})$
1700vs	1720s	1780vs	$\nu_{\text{asym}}(\text{C}=\text{O})$
1620w	1610w	1610w	$\delta(\text{HOH})$
–	1600–1540vs	1600–1530vs	$\nu(\text{COO})$ carboxylate
1430, 1380s	1440–1390vs	1400vs	$\nu_{\text{sym}}(\text{COO})$
1240–1190s	1250–1190s	1300–1200s	$\nu_{\text{sym}}(\text{C}-\text{O})$
1080–1050s	1130–1050s	1070w	Citrate
940, 900sh	900br	930, 890w	Citrate
780sh	800br	800–780br	Citrate
600sh	600br	600br	Citrate

s, Strong; vs, very strong; sh, shoulder; br, broad; m, medium; w, weak.

TABLE 3  
IR spectral frequency assignments for  $Dy_3Fe_5(Cit)_{25} \cdot (36+n)H_2O$  and decomposition products

Dy precursor	Heat treatment temperature (°C)							Assignment
	170	280	330	450	600	700	750	
3700-3000vs	3700-3000vs	3650-3000s	3600-3000s	3600-3270s	3600-3300m	3400br	3400w	$\nu(OH)$ water
2900s	2900w	-	-	-	-	-	-	$\nu(CH)$
-	-	2320w	2320w	2320w	-	-	-	$\nu(CO_2)$
1700vs	1700s	-	-	-	-	-	-	$\nu_{asym}(C=O)$
1610w	1610w	1610w	1610w	1610w	1610vw	1610vw	1610vw	$\delta(HOH)$ water
1570s	1570s	1570s	-	-	-	-	-	$\nu_{asym}(COO)$ carboxylate
-	-	-	1500vs	1500w	-	-	-	$\nu(CO)$ carbonate
1400vs	1400s	1400s	1400vs	1400w	-	-	-	$\nu_{sym}(COO)$ or $\nu_{sym}(CO)_3$
1250s	1250m	-	-	-	-	-	-	$\nu_{sym}(C-O)$
-	-	1070w	1070w	1070vw	-	-	-	$\nu_{sym}(C-O)$ carbonate
-	-	-	-	1130br	1130s	1130s	1130vs	Overtones of lattice modes
-	-	-	-	-	860, 910m	860, 910sh	860, 910sh	Lattice modes
-	-	840m	840m	840w	-	-	-	$\pi(CO_3)$
800, 730s	800, 730m	-	-	560br	560, 600br	560, 600br	560m, 600, 660vs	Citrate absorption
-	-	-	-	-	-	-	-	$\nu_3(FeO_4)$ of garnet

s, Strong; vs, very strong; sh, sharp; m, medium; w, weak; br, broad.



ing mode of water at  $1610\text{ cm}^{-1}$  disappears as the heat treatment temperature increases. The absorptions of the citrate precursor at 1700, 1570, 1400 and  $1250\text{ cm}^{-1}$  are assigned in Table 3. The 1700 and  $1250\text{ cm}^{-1}$  absorptions disappear above  $200^\circ\text{C}$  retaining only the two carboxylate absorptions at 1570 and  $1400\text{ cm}^{-1}$  up to  $275^\circ\text{C}$  [7]. This shows that although the basic citrate structure has broken down by  $275^\circ\text{C}$ , some carboxylate groups still remain and give rise to the above two  $\nu(\text{COO}^-)$  absorptions. The absorption at  $1570\text{ cm}^{-1}$  is a broad band and disappears above  $330^\circ\text{C}$ , but the strong band at  $1400\text{ cm}^{-1}$ , composite band which corresponds to carbonates, also decreases in intensity after  $400^\circ\text{C}$  and eventually disappears above  $500^\circ\text{C}$ . A longer heat treatment at  $450^\circ\text{C}$  for more than 20 days removes this band. The spectrum at  $330^\circ\text{C}$  and above shows broad complex carbonate bands at 1500, 1400 and  $1070\text{ cm}^{-1}$ . The band at  $1070\text{ cm}^{-1}$  is only weakly active and the deformation mode occurs at  $840\text{ cm}^{-1}$ . The spectrum of the intermediate carbonate  $\text{Dy}_3\text{Fe}_5\text{O}_6(\text{CO}_3)_6(\text{CO}_2)_3$  has, in addition to the carbonate bands, a band at  $2350\text{ cm}^{-1}$  which must be due to the asymmetric stretching mode of free carbon dioxide, as reported elsewhere [6]. The sharp absorptions at 860 and  $910\text{ cm}^{-1}$  and the strong broad absorptions at  $500\text{--}700\text{ cm}^{-1}$  are due to lattice absorptions in  $\text{Dy}_3\text{Fe}_5\text{O}_{12}$  [8,9]. There is a broad absorption band in the region  $1100\text{--}1200\text{ cm}^{-1}$  at higher temperatures which corresponds to the overtones or combinations of the fundamental modes of the  $\text{Dy}_3\text{Fe}_5\text{O}_{12}$  phase. The increase in intensity of the above bands with temperature is understood in terms of the manifestation of  $\text{Dy}_3\text{Fe}_5\text{O}_{12}$  phase.

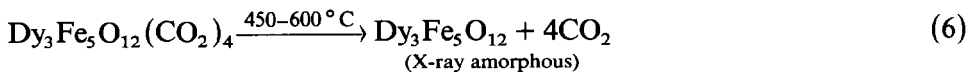
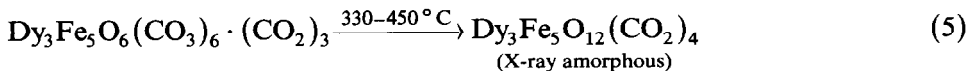
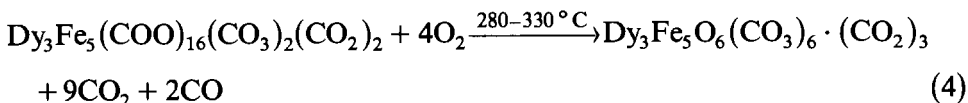
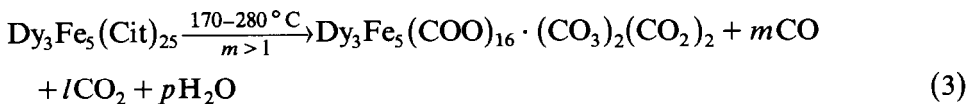
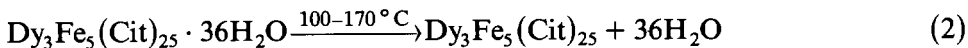
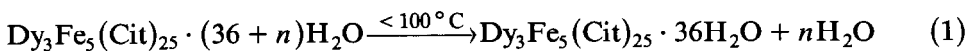
### *Proton NMR spectral studies*

The anhydrous citric acid spectrum [10] has a resonance at  $\delta = 2.7$  due to the methylene protons and a weak hydroxyl peak appearing as a shoulder at  $\delta = 2.5$ . The carboxylic acid protons give a broad peak at  $\delta = 11.0$ . The anhydrous dysprosium iron citrate precursor has a strong methylene proton peak at  $\delta = 2.0$  and a hydroxyl peak at  $\delta = 2.5$  with an integrated intensity ratio of 4 : 1, without any carboxylic acid proton peaks. Citric acid bonding with  $\text{Dy}^{3+}$  and  $\text{Fe}^{3+}$  should have its methylene peak at higher  $\delta$  values if these ions are electron-withdrawing in nature. But it is observed at lower  $\delta$  values. The  $=\text{CH}_2$  protons appear at higher values of  $\delta = 3.0$  in the monosodium salt of citric acid, because of the electron-withdrawing nature of the  $\text{Na}^+$  [10]. Hence, the shift towards lower  $\delta$  values of the methylene protons peak in citrate precursor shows that the bonding is different from that of the monosodium salt of citric acid. The presence of a hydroxyl peak in the spectrum shows that the hydroxyl group does not take part in bonding. The citrate precursor heat-treated at and above  $190^\circ\text{C}$  does not show a methylene proton peak indicating that these protons have been burnt off at this temperature. The samples decomposed at higher temperatures (above  $190^\circ\text{C}$ )

do not show any proton NMR spectra because the hydrogen atoms from the methylene and hydroxyl groups have been burnt off.

## DISCUSSION

To propose a mechanism for the thermal decomposition, a knowledge of the initial citrate gel structure would be useful. However, very little evidence is available in the literature concerning the possible structural arrangements within the citrate gels. Brinker and Scherer [11,12] have proposed that the extent of polymerization in the gel is dependent on pH. At lower pH values, the extent of polymerization in the gel is not sufficient to form a network of solid structures and, in fact, the dysprosium iron citrate gel is obtained in the pH range 1–3 in these studies. Moreover, Spaulding and Brittain [13], in their study of lanthanide complexes of citric acid, have observed that the number of citric acid molecules coordinating with trivalent lanthanide ions could be between 1 and 5, that is  $\text{Ln}(\text{Cit})\text{--}\text{Ln}(\text{Cit})_5$ , depending upon the conditions and the individual rare earth ions. Thus, it is difficult to predict the number of citric acid molecules associated with the metallic ions. Therefore, the plausible mechanism is proposed on the basis of thermal analyses, gas analysis, IR and NMR data. Dysprosium iron citrate precursor decomposes to  $\text{Dy}_3\text{Fe}_5\text{O}_{12}$  phase. The experimental results indicate the following scheme



The first step represents the removal of extra water absorbed by the citrate precursor. The second step in the decomposition of the citrate precursor corresponds with the loss of coordinated water. The third step corresponds to the main decomposition of citrate with evolution of carbon

monoxide gas, carbon dioxide gas and water due to burning of the methylene groups. The residue at this decomposition step has only an apparent composition and cannot be isolated with fixed stoichiometry. In the fourth step, complete conversion of all the carboxylates to carbonates take place, which can be observed by the disappearance of the  $1570\text{ cm}^{-1}$ ,  $\nu_a(\text{COO}^-)$  absorption band in the IR spectrum and the appearance of a stronger  $1500\text{ cm}^{-1}$  band due to complex carbonates. The gas evolved is mainly carbon dioxide, as confirmed by the gas analysis data. Some amount of carbon dioxide gas gets trapped in the lattice, which can be seen from the  $2330\text{ cm}^{-1}$  absorption in the IR spectrum. The fifth step represents the decomposition of all carbonates culminating in the formation of DyIG with small amounts of residual carbon and trapped  $\text{CO}_2$  gas molecules. This compound is found to be X-ray amorphous. The carbon residuals disappear only on keeping the samples above  $450^\circ\text{C}$  for more than 20 days. Finally, the crystallization of amorphous garnet takes place at  $590^\circ\text{C}$ , which is shown in Fig. 3 by an exotherm on the thermogram. The XRD pattern shows a broad characteristic band for the crystalline (DyIG) garnet phase. The crystallized DyIG has a particle size of  $160\text{ \AA}$  from X-ray line-width measurements [14]. A surface area of  $60\text{ m}^2\text{ g}^{-1}$ , measured by the BET method for the crystallised DyIG, corresponds with a particle size of  $150\text{ \AA}$ .

It may be noted that the weight loss measurements in TG and the explanations based on these results are definitely limited in scope and the intermediates need not represent stable compositions. Moreover, thermoanalytical methods, such as TG, which are dynamic processes, are not suitable for the determination of the compositions of intermediates. The compositions of the residues isolated from the isothermal experiments need not, and often do not, tally with the apparent compositions assigned by weight loss measurements during thermal analyses.

## CONCLUSIONS

The synthesis of amorphous and crystalline  $\text{Dy}_3\text{Fe}_5\text{O}_{12}$  garnets by the citrate gel process was investigated and the mechanism of the thermal decomposition was examined in detail. The chocolate-coloured flaky dysprosium iron citrate precursor is obtained on drying the citrate gel at  $100^\circ\text{C}$  and is found to have the formula  $\text{Dy}_3\text{Fe}_5(\text{Cit})_{25} \cdot 36\text{ H}_2\text{O}$ . The citrate precursor absorbs 5–15% water depending on the atmospheric humidity. Air atmosphere is found to be most suitable for the decomposition process, which results in the growth of pure stoichiometric DyIG phase. The thermal decomposition process of the citrate precursor consists of three major steps: dehydration, decomposition of citrate groups to carbonates and decomposition of the carbonate yielding amorphous DyIG at  $450^\circ\text{C}$ . The high decomposition rate, low decomposition temperature and dissipation of heat

by the large amount of gases evolved results in the formation of X-ray amorphous DyIG with a crystallite size of 11–14 Å, existing as clusters of 300 Å which are evident from surface area measurements.

#### REFERENCES

- 1 D.W. Johnson, Jr., *Am. Ceram. Soc. Bull.*, 60 (1981) 221, 243.
- 2 Ch. Marcilly, P. Courty and B. Delmon, *J. Am. Ceram. Soc.*, 53 (1970) 56.
- 3 M.S. Multani, D.K. Sharma, V.R. Palkar, S.G. Gokarn and A. Gurjar, *Mater. Res. Bull.*, 16 (1981) 1535.
- 4 Ph. Courty, H. Ajot, Ch. Marcilly and B. Delmon, *Powder Technol.*, 7 (1973) 21.
- 5 Th.J.A. Popma and A.M. van Diepen, *Mater. Res. Bull.*, 9 (1974) 1119.
- 6 H.S.G.K. Murthy, M. Subba Rao and T.R. Narayanan Kutty, *J. Inorg. Nucl. Chem.*, 37 (1975) 891.
- 7 R. Nakamoto, *Infrared and Raman Spectra of Inorganic and Coordination Compounds*, John Wiley, New York, 1978.
- 8 N.T. McDevitt, *J. Opt. Soc. Am.*, 59 (1968) 1240.
- 9 D.L. Wood, J.P. Remeika, *J. Appl. Phys.*, 38 (1967) 1038.
- 10 C.J. Pouchart (Ed.), *The Aldrich Library of NMR Spectra*, Edition II, vol. 1, No. 458D and No. 459B.
- 11 C.J. Brinker and G.W. Scherer, *J. Noncryst. Sol.*, 70 (1985) 301.
- 12 C.J. Brinker and G.W. Scherer, in L.L. Hench and D.R. Ulrich (Eds.), *Ultrastructure Processing of Ceramics, Glass and Composites*, John Wiley, New York, 1985, p. 43.
- 13 L. Spaulding and H.G. Brittain, *J. Lumin.*, 28 (1983) 385.
- 14 H.P. Klug and L.P. Alexander, *X-ray Diffraction Procedures*, Ch. 9, Wiley, New York, 1954.